Theoretical Study of Binding of Hydrated Zn(II) and Mg(II) Cations to 5′-Guanosine Monophosphate. Toward Polarizable Molecular Mechanics for DNA and RNA

Nohad Gresh,*,† Judit E. Šponer,‡ Nad'a Špačková,‡ Jerzy Leszczynski,§ and Jiři Šponer⊥,‡,§

Laboratoire de Pharmacochimie Moléculaire et Structurale, FRE 2463 CNRS, U266 INSERM, Faculté de Pharmacie de Paris, Université René-Descartes, 4, Avenue de l'Observatoire, 75006 Paris, France, Institute of Biophysics, Academy of Sciences of the Czech Republic, National Center for Biomolecular Research, Kralovopolská 135, 612 65 Brno, Czech Republic, Department of Chemistry, Computational Center for Molecular Structure and Interactions, Jackson State University, Jackson, Mississippi 39217, and J. Heyrovsky Institute of Physical Chemistry, Academy of Sciences of the Czech Republic, Dolejskova 3, 182 23, Prague

Received: December 30, 2002; In Final Form: May 19, 2003

SIBFA polarizable molecular mechanics (PMM) and quantum-chemical (ab initio Hartree−Fock and DFT) computations are performed on the binding of hydrated Zn(II) and Mg(II) cations to 5′-guanosine monophosphate, a basic building block of nucleic acids, probing both C2′ endo and C3′ endo conformations. The interaction energies of the hydrates, ΔE_{int}, are compared in three distinct arrangements: (**A**) simultaneous binding of the dication to both O1 and N7, (**B**) direct binding to O1 and through-water binding to N7, and conversely, (**C**) through-water binding to O1 and direct binding to N7. With a C2′ endo sugar, bidentate complex **A** has a marginally more favorable ΔE_{int} than directly bound phosphate complex **B**. With a C3′ endo sugar, **A** has a distinctly more favorable ΔE_{int} value than **B** and **C**. ΔE_{int}(SIBFA) has values that are intermediate between those of ΔE(DFT) obtained using the 6-311G** and LACVP** basis sets. Zn(II) complexes are favored over the corresponding Mg(II) ones by the dispersion and charge-transfer terms, while the sum of electrostatic and short-range repulsion favors the Mg(II) complexes. The different balance of individual contributions is responsible for the distinct biological and biochemical roles of the two cations. Additional comparisons of PMM with quantum-chemical computations are performed for the solvation energy, ΔG_{solv}, computed with a continuum reaction field procedure integrated in SIBFA, and for the internal conformational energy of the nucleotide in the investigated complexes. The SIBFA and quantum-chemical results are also compared with polarizable and nonpolarizable force fields currently available in the AMBER molecular modeling code.

Introduction

Divalent cations have a prominent role in stabilization of DNA and RNA molecules. There is mounting evidence that divalent cations are involved in stabilization of certain key tertiary contacts in RNA and extended non-Watson−Crick RNA regions in a highly specific manner. Divalent cations also intervene as cofactors for RNA-mediated catalysis. The structural role of Mg(II) cations was evidenced for the first time in 1977 by high-resolution X-ray crystallography of tRNA.[1] Although the following list does not attempt to be a complete one, outstanding examples of atomic resolution data on RNA−divalent cation interactions are provided by the hammerhead ribozyme,[2] intron ribozymes,[3] lead-dependent ribozymes,[4] spliceosomal RNA,[5] and viral pseudoknots.[6] One of the most stunning cases is the 5S rRNA Loop E bacterial RNA motif, a 7-base-pair non-Watson−Crick region stabilized in the crystals by a string of 4−5 Mg(II) cations interacting with the major (deep) groove.[7] Although many of the metals seen in the crystal structures are due to crystallization conditions and are primarily involved in lattice contacts, at least some of them represent structurally and functionally relevant binding. The role of metals in nucleic acids is clearly evidenced also by other experimental techniques.[8]

On the DNA side, recently a pivotal role was suggested for divalent cations in DNA-mediated catalysis (DNA-zymes[9]). Processing of DNA is done by metalloenzymes having a mono- or a binuclear metal center.[10] Stabilization of antiparallel[11] and parallel[12] DNA triple-helical sequences was demonstrated to occur in the presence of Zn(II), while Mg(II) was not effective for some sequences.[12,13]

Due to their transient nature, the complexes between divalent cations and nucleic acids can be very difficult to isolate and structurally characterize. It is also not always straightforward to distinguish metal cations bound to biologically relevant position and cations related primarily to the crystallization process and the crystal unit. More importantly, while crystals clearly show the molecular structures, they do not reveal the nature and energies of the interactions. Thus, a substantial piece of information is missing, and the crystal data can sometimes be misinterpreted. For example, there has been recent speculation about the role of a novel cation−π interaction in the B-DNA crystal of d(CGCGAATTCGCG)$_2$ involving hexahydrated Mg(II) and cytosine bases.[14] Two subsequent ab initio quantum-chemical studies did not find any such interactions and explained the observed binding entirely as the conventional major groove binding of magnesium hexahydrate to guanine bases.[15] It is thus

* Corresponding author. E-mail: gresh@citi2.fr.
† Université René-Descartes.
‡ Institute of Biophysics, Academy of Sciences of the Czech Republic.
§ Jackson State University.
⊥ J. Heyrovsky Institute of Physical Chemistry, Academy of Sciences of the Czech Republic.

10.1021/jp022659s CCC: $25.00
Published on Web 07/22/2003

very tempting to complement the existing experimental techniques by using advanced computational tools, since these methods are able to address the fundamental links between biomolecular structures and energies.

DNA and RNA molecules are now widely studied by nanosecond-scale molecular dynamics (MD) simulations with explicit inclusion of solvent and ions.[16] Naturally, MD simulations were also used to characterize the interactions of nucleic acids with cations, such as penetration of monovalent cations to B-DNA grooves,[17] formation of high-occupancy sodium binding sites in complex RNA shapes such as the frameshifting pseudoknot and 5S rRNA Loop E,[18] cation stabilization of guanine quadruplex molecules (G-DNA), which has been extensively studied,[19] and interaction of Mg(II) with the active site of hammerhead ribozyme[20] and platinated DNA duplex.[21] However, the conventional pair-additive force fields currently used in all atom MD simulations are substantially deficient in their ability to describe interactions between metal cations and nucleic acids. The force field parametrization of metal cation interactions is inevitably the least reliable part of the force field.[22] Obviously, the force field shows the best performance for monovalent cations such as Na(I). Nevertheless, even here defects such as local deformations of G-DNA guanine tetrads have been noticed and ascribed to the pair-additive nature of the force field.[19a] A recent X-ray study revealed stable binding of K(I) to the diagonal loop of the $d(GGGGTTTTGGGG)_2$ quadruplex,[23] which seems to be very difficult to reproduce via contemporary MD simulations.[19b] For divalent species such as Mg(II) and Zn(II), the quality of the force field predictions worsens dramatically. The magnitude of nonadditive contributions in the first coordination shell of divalent cations is ca. 50−100 kcal/mol; these contributions are, by definition, omitted from the force fields. The nonelectrostatic (polarization and charge-transfer) terms decisively contribute to selectivity of cation binding to nucleic acids. Simulations of DNA or RNA complexes with divalent cations remain an uncharted ground. The large size of the biomolecular systems and the long-range nature of ionic interactions hamper, on the other hand, a straightforward use of conventional quantum-chemical approaches. Thus, development of efficient polarizable molecular mechanics (PMM) is of primary importance (see ref 24 for a recent review).

We previously developed the SIBFA polarizable mechanics procedure on the basis of ab initio computations[25] and tested it by comparisons to the latter in several polycoordinated complexes of divalent cations[26] and multiply hydrogen-bonded complexes.[27] It was applied to study complexes between inhibitors and Zn−metalloenzymes,[28] and to a Zn-finger from an HIV-1 nucleocapsid.[29] In another recent investigation, we reported the results of parallel SIBFA and quantum-chemical studies of the complexes between pentahydrated Zn(II) and guanine, adenine, and the G−C and A−T base pairs.[30] The SIBFA PMM was capable to reproduce all major trends seen in the ab initio analysis at a fraction of the computational cost, including an effect known as polarization enhancement of base-pairing stability by metal binding. The present study constitutes an extension of the preceding work to the complete basic RNA building block, guanosine monophosphate ($5'GMP^-$). It follows and extends our preliminary ab initio analysis of metal−nucleotide systems.[31]

The options for binding of a hexacoordinated divalent metal cation to $5'GMP^-$ are highly variable and include both inner- and outer-shell binding to the solute atoms. The leading cation binding sites are the N7 guanine position, offering a broad negative electrostatic potential, and the lone pair, which is able to interact with the metal cation d electrons, the anionic phosphate oxygens, and also the guanine O6 atom. Interaction with other atoms, such as N3(G) or the sugar, is not ruled out but is much less likely. As is well documented in the X-ray structures, the cations may adopt a wide range of binding, including simultaneous binding to several sites within the nucleotide. In nucleic acids, binding of a hydrated cation may involve positions belonging to two consecutive nucleotides or intermediate intermolecular contacts. The ribose could adopt a C2′ endo or a C3′ endo puckering, and the repuckering also can be related with the type of cation binding. The C2′ endo and C3′ endo sugar puckerings are characterized by pseudorotational phases of ca. 144−180° and 0−36°, respectively, and amplitude values in the 25−50° range. The PMM force field must provide a balanced description of all binding possibilities and properly account for differences in binding of various cations to distinct binding sites. Obviously, the distribution of binding patterns in various types of nucleic acids may differ from those investigated for nucleotide−metal complexes. Nevertheless, it is fair to assume that once a PMM is able to reproduce the reference ab initio data for a wide range of nucleotide−metal binding motifs, it also provides a reliable description of metal−nucleic acid interactions. Thus, the nucleotide−metal cation system is the genuine complex for the evaluation of PMM.

Here we present quantum-chemical (Q-C) and SIBFA analyses of $5'GMP^-$−hydrated metal cation complexes, providing new insights into important aspects of metal−nucleic acid binding. We further evaluate the ability of SIBFA computations to study these systems regarding the following four aspects:

(i) Intermolecular interaction energies and their evolutions in competing binding modes.

(ii) Variations in the intramolecular (conformational) energy of $5'GMP^-$, δE_{conf}.

(iii) Evaluation of hydration energies, ΔG_{solv}. In simulations of nucleic acids, the use of continuum reaction field procedures to compute solvation energies can be necessary.[32] Thus, we compare the values of ΔG_{solv} of complexed and uncomplexed $5'GMP^-$ in the different arrangements using several approaches. First, in the context of PMM methods, we use the Langlet−Claverie[33] procedure integrated in the SIBFA software.[34] We then use a QC-based DFT procedure coupled with the Poisson equation[35] and also the polarizable charge model as described by Tomasi et al.[36] This is the first time such ΔG_{solv} evaluations have been done in studies of metal binding to nucleic acids.

(iv) Finally, we identify energy components that differentiate between Zn(II) and Mg(II) binding. Issues such as Zn(II) vs Mg(II) selectivity are entirely beyond the capability of conventional pair-additive force fields that treat cations as van der Waals spheres with a point charge in their centers and cannot be properly handled, even with simplified polarizable force fields still neglecting charge transfer.

Procedure

Molecular Mechanics. In the SIBFA procedure,[25] the intermolecular interaction energy, ΔE_{int}, is computed as the sum of five separate contributions:

$$\Delta E_{int} = E_{MTP} + E_{rep} + E_{pol} + E_{ct} + E_{disp}$$

with electrostatic multipolar (E_{MTP}), short-range repulsion (E_{rep}), polarization (E_{pol}), charge-transfer (E_{ct}), and dispersion (E_{disp}). The multipoles (up to quadrupoles) are distributed on the atoms

and bond barycenters using a procedure developed by Vigné-Maeder and Claverie.[37] The anisotropic polarizabilities are distributed on the centroids of the localized orbitals (heteroatom lone pairs and bond barycenters) using a procedure attributed to Garmer and Stevens.[38] We denote below by E_1 the sum of the first-order components, E_{MTP} and E_{rep}, and by E_2 the sum of second-order components, E_{pol} and E_{ct}.

The intramolecular energy, E_{intra}, in a flexible molecule is computed as a sum of intermolecular interaction energies between the fragments making up the molecule, using the same components and formulation as ΔE_{int}. The fragments making up the guanosine part of 5′GMP$^-$ are guanine, deoxyribose prefixed in standard geometries corresponding to C2′ or C3′ endo conformation, and two water-like fragments to account for the 2′ and 3′ OH substituents. The methyl phosphate part of 5′GMP$^-$ is constructed from four elementary fragments: water, $H_2PO_4^-$, water, and methane, having the same geometries as in methyl phosphate. The multipoles and polarizabilities are those of the fragments taken in isolation, and not those extracted from methyl phosphate. This choice follows the conclusion of our recent study,[39] which was devoted to the binding of divalent cations to the triphosphate anion, a key constituent of ATP and GTP. This study showed that a close reproduction of the conformation-dependent ab initio Hartree−Fock (HF) and MP2 interaction energies was possible if the anion was built from such basic mutually interacting fragments (including in that case a terminal HPO_3^{2-} fragment), the interactions of which are computed simultaneously with those involving the external molecules. In the course of the present work, we had initially resorted to multipoles extracted from a methyl phosphate anion, subsequently redistributed on the four elementary fragments to allow for rotations along the three junctional bonds. In such a case, however, while the ΔE_{int} values were found to be close to the Q-C ones, the conformational energies, δE_{conf}, of 5′GMP$^-$ were in some cases overestimated with respect to the corresponding Q-C ones. This was traced back to a corresponding imbalance of the intra-phosphate interactions. This translated the fact that the molecular orbitals (MOs) of integral methyl phosphate embody the effects of electron redistribution over the whole molecule, which took place during the iterative SCF process. Therefore, the multipoles derived from these MOs have already built into them the effects of mutual interactions between the constituent atoms of methyl phosphate. Such multipoles, therefore, should not be used to compute the intramolecular energy as a sum of its fragment−fragment interaction energies, since this would amount to double-counting. Instead, the electrostatic component of these interactions should resort to the multipoles of the unperturbed (isolated) constitutive fragments.

The fragment multipoles and polarizabilities were derived from ab initio computations using the CEP 4-31G(2d) basis set.[40] In addition, E_{intra} embodies a three-fold torsional term (E_{tor}) along the C−C and C−O bonds, having V_0 amplitudes of 2.3 and 1.5 kcal/mol, originally fitted to reproduce the torsional barriers of ethane and ether.[25a]

To allow for the simultaneous computation of intra- and intermolecular interactions, we have applied a new procedure tested on the intramolecular (conformational) energies of Ala tetrapeptides, validated by ab initio results (Gresh et al., submitted), and recently used in studies of Zn-fingers of the HIV-1 nucleocapsid.[29] As in the initial SIBFA treatment,[25a] the new procedure redistributes the multipoles at the junctions between fragments to compute E_{MTP}. On the other hand, to compute E_{pol}, the multipoles are not redistributed, but rather the junctional H atoms are carried back on the C, N, or O atoms whence they originate. This procedure prevents the fragments from acquiring a non-net fractional charge following multipole redistribution, which could locally exaggerate the value of E_{pol}, and from being at short distances from the junctional H atoms. The polarizabilities on the junction bonds were set to zero. This was done in order to prevent possible divergences of E_{pol} on account of the short distances between each junction center and the polarizable centers of the connected fragments. Within this procedure, the interactions involving Zn(II) and the waters with 5′GMP$^-$ as well as between themselves are included, simultaneously with the intranucleotide interfragment interactions, in the computation of the total E_{intra}. In the results discussed below, the total interaction energy, ΔE_{int}, and its components are derived as the differences between the total E_{intra} energies or components thereof and those in the absence of Zn(II) and the waters at the same conformation. The need for a simultaneous and consistent computation of inter- and intramolecular polarization and charge-transfer components on account of their nonadditive character was recently underlined.[41]

Energy minimization was performed on the set of torsional angles of 5′GMP$^-$ and each set of six/three variables defining the approach of the water/Zn cation to the nucleotide. It used the "Merlin" minimizer.[42]

The solvation energies are computed using the Langlet−Claverie procedure[33] interfaced in SIBFA.[34] This procedure uses the same ab initio distributed multipoles as the SIBFA procedure, ensuring mutual consistency. The van der Waals (vdW) surface of the cavity was multiplied by a factor of 1.2. In previous studies,[26a,28,34] the factor was 1. We have accordingly reparametrized the exponent of the exponential of the repulsion energy, and the multiplicative factors of the repulsion and of the dispersion energy terms. These three parameters now have the values 11.40, 28780.0, and 0.29, respectively. We have adopted a multiplicative factor of 1.2 for the vdW cavity on the basis of simulations on small and partly unshielded complexes of divalent cations, which with a 1.0 factor tended to dissociate in the presence of the continuum to expose a bare divalent cation.

Quantum-Chemical Computations. The energy decomposition analyses used the restricted variational space (RVS) analysis method described by Stevens and Fink,[43] using the CEP 4-31G(2d) basis set. The corrections for the basis set extension error (BSSE) are done with the virtual orbital basis set.[44] The RVS analyses are complemented with MP2 computations to get the contribution of correlation, E_{corr}, to the interaction energy.[45] RVS and MP2 computations used the GAMESS package.[46]

DFT computations used the B3LYP functional[47] and the 6-311G** and the LACVP** [48] Gaussian basis sets. These computations were done with the Gaussian[49] and Jaguar[50] packages.

The calculations of the continuum solvation energies were done using the Poisson equation within the DFT procedure[35] or the PCM procedure described by Tomasi et al.[36]

Ab initio calculations were carried out at the HF level of theory as implemented in the Gaussian98 program package.[49] Gradient optimizations, starting from the SIBFA-optimized structures, were carried out using the 6-31G* basis set on the Mg, C, H, N, and O atoms. For the two anionic oxygens interacting with the $[M(H_2O)_5]^{2+}$moiety (M = Zn, Mg), this basis set was augmented with an sp-type diffuse shell (exponent 0.0845). The Zn atom was described by the pseudopotential identified by Christiansen et al.[51] In a subsequent step we computed single-point energies for the HF/6-31G* geometries

TABLE 1: RVS Energy Decomposition, MP2/DFT Correlated Energies, and SIBFA Calculations on Model Complexes of $[Zn(H_2O)_5]^{2+}$ with the Methyl Phosphate Anion

	direct Zn-phosphate binding				through-water Zn-phosphate binding			
	A(a)[a]		**B**(b)[b]		**C**(c)[c]		**C**(d)[d]	
	RVS/HF	SIBFA	RVS	SIBFA	RVS	SIBFA	RVS	SIBFA
E_1	−363.9	−382.8	−357.1	−385.7	−325.9	−338.0	−332.6	−349.4
E_{pol}		−86.2		−96.3		−97.1		−94.7
E_{pol}* [e]		−103.0		−116.2		−114.4		−112.8
E_{polRVS}	−117.9		−130.1		−122.5		−122.3	
E_{ct}	−25.9	−27.5	−31.2	−29.1	−28.7	−29.4	−29.0	−29.7
ΔE_{RVS}	**−486.8**		**−494.3**		**−458.7**		**−465.0**	
ΔE		**−496.6**		**−511.0**		**−464.5**		**−473.8**
ΔE(i)[f]	**−485.3**		**−492.1**		**−457.8**		**−462.1**	
ΔE(ii)[g]	**−510.6**		**−519.9**		**−483.7**		**−488.5**	
	MP2, CEP 4-31G(2d) Basis Set							
	MP2	SIBFA	MP2	SIBFA	MP2	SIBFA	MP2	SIBFA
E_{corr}	−41.2		−42.7		−38.0		−38.7	
E_{disp}		−39.4		−49.6		−38.0		−41.9
ΔE_{int}	**−528.0**	**−535.9**	**−537.0**	**−560.6**	**−496.7**	**−502.4**	**−503.7**	**−515.8**
	DFT Using 6-311G** and LACVP** Basis Sets							
	DFT	SIBFA	DFT	SIBFA	DFT	SIBFA	DFT	SIBFA
ΔE_{int}(i)	**−517.4**	**−535.9**	**−525.8**	**−560.6**	**−490.7**	**−502.4**	**−495.8**	**−515.8**
ΔE_{int}(ii)	**−547.5**		**−558.3**		**−521.5**		**−527.1**	

[a] (a), from complex **A**, defined below, with Zn(II) bridging N7 and O1. [b] (b), from complex **B**, with Zn(II) bound to O1. [c] (c), from complex **C**, with Zn(II) bound to N7 and through water to O1. Deoxyribose in the C2′ endo conformation. [d] (d), from complex **C**, with Zn(II) bound to N7 and through water to O1. Deoxyribose in the C3′ endo conformation. [e] Without the contributions of the induced dipoles to the polarizing field. [f] (i), 6-311G** basis set. [g] (ii), LACVP** basis set.

using the 6-311+G** basis set of atomic orbitals on the C, H, N, and O atoms. These calculations were done at both the HF and DFT/B3LYP levels of theory. For some selected structures, we also performed a HF geometry optimization with the 6-311+G* basis set.

Results and Discussion

As a starting point for this study, we have resorted to the structure of the complex formed between 5′GMP$^-$ and a pentahydrate of Zn(II) derived from HF gradient energy minimization. In this structure, Zn(II) was directly bound to N7, and bound to two anionic oxygens O1 through two water molecules. The sugar was in the C2′ endo conformation. With the help of computer graphics, this structure was then modified to allow for either simultaneous and direct Zn(II) binding to both O1 and N7, or to direct binding to O1 and through-water binding to N7. Related structures were generated in which the ribose was held in the C3′ endo conformation. These structures were then subjected to energy minimization using SIBFA. Subsequently, **A** will denote the structures having Zn(II) bound directly to both O1 and N7, **B** those having Zn(II) bound directly to O1 and through-water to N7, and **C** those having, conversely, Zn(II) bound directly to N7 and through-water to O1.

$[Zn(H_2O)_5]^{2+}$ Complexes. We report in Tables 1−3 the results on the computations on the $[Zn(H_2O)_5]^{2+}$ complexes with the methyl phosphate anion and with 5′GMP$^-$. The interaction energies, ΔE_{int}, are computed as the difference between the energy of the complex and the energies of the monomers in isolation. The energy of the flexible ligand, 5′GMP$^-$, is computed in the conformation it adopts in the complex considered. Except for the RVS computations, the values of ΔE_{int} are not corrected for the BSSE. This contribution is relatively small for ionic systems. It is thus less than 4 kcal/mol out of 500, i.e., 1%, in the $[Zn(H_2O)_5]^{2+}$−methyl phosphate complexes reported below.

1. $[Zn(H_2O)_5]^{2+}$−Methyl Phosphate Complexes. Before introducing the data on nucleotide−metal interactions, let us present a series of reference calculations on binding of $[Zn(H_2O)_5]^{2+}$ to the anionic moiety of 5′GMP$^-$, i.e., the methyl phosphate (Table 1). The purpose of these model computations was two-fold. First, we evaluated, by comparisons with the RVS energy-decomposition analysis, the extent to which the numerical values of the individual components of ΔE(RVS), E_1, E_{pol}, and E_{ct}, are accounted for in SIBFA PMM. The RVS decomposition is not feasible for the nucleotide complexes but is of critical importance to understand the balance of the interactions. Further, the data reveal the sensitivity of the computed results to configuration, notably when comparing direct (inner-shell) and through-water (outer-shell) binding of Zn(II) to the phosphate. Second, we assessed the basis set sensitivity of ΔE and the mutual consistency between DFT and MP2 data. Analogous reference data for metal−guanine interaction were published in our preceding study.[30] For that purpose, single-point energy computations were performed on four representative structures extracted from the 5′GMP$^-$−$[Zn(H_2O)_5]^{2+}$ complexes (Figure 1, (a)−(d)). Zn(II) binds directly to the anionic O1 atom of phosphate in modes (a) and (b), that were taken from the full complexes **A** and **B**, assuming the C3′ endo sugar pucker. Modes (c) and (d) were extracted from complexes **C** (direct binding of Zn(II) to N7), with the ribose C2′ endo and C3′ endo, respectively.[52] The first comparisons of direct versus through-water binding of a hydrated divalent cation, Mg(II), were reported by Pullman et al.[53]

The RVS analysis was undertaken using the CEP 4-31G(2d) basis set, which was, consistent with our previous studies,[25−28,30] used to derive the SIBFA multipoles and polarizabilities. Along with this analysis, MP2 computations are carried out in order to evaluate the extent to which the interaction energy gains resulting from correlation can be reproduced by the E_{disp}

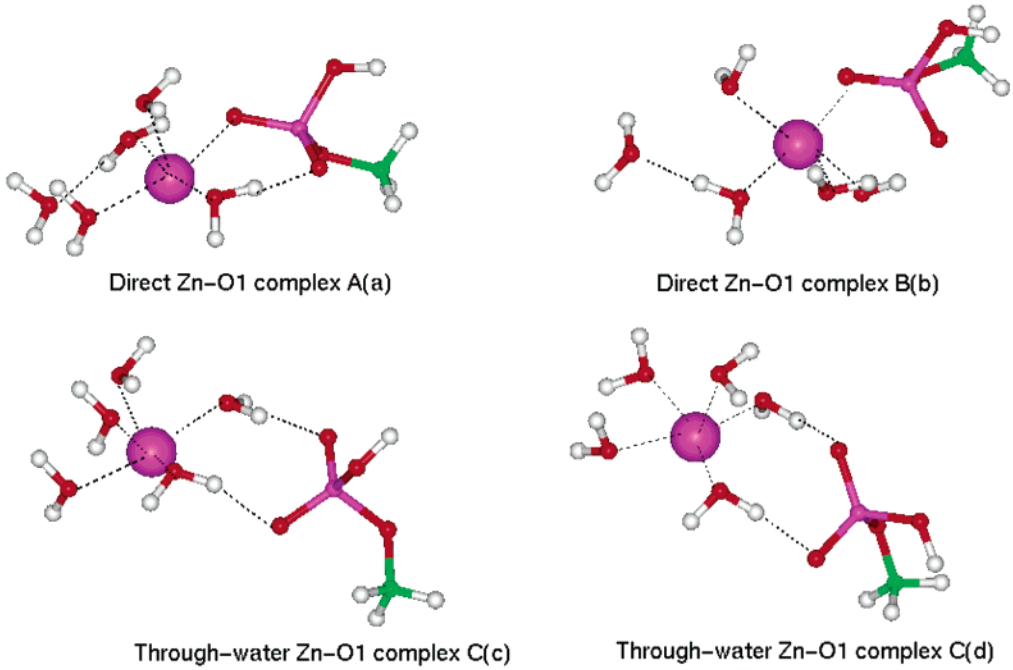

Figure 1. (a)−(d) Representation of the complexes of $[Zn(H_2O)_5]^{2+}$ with phosphate. (a),(b) Direct Zn(II) binding to O1. (c),(d) Through-water binding.

component from SIBFA. The above computations are complemented by additional ones using the 6-311G** and LACVP** [48] basis sets. These basis sets were previously used by us in studies of polyligated guanine complexes of divalent cations[30] and complexes of inhibitors with active sites of metalloenzymes.[28b] Both HF and DFT computations have been performed, enabling comparisons to be performed at the correlated level between MP2/CEP 4-31G(2d) and DFT ΔE values.

At the HF level, we see the following order of stabilization:

$$(b) > (a) > (d) > (c)$$

which is reproduced by SIBFA. An analysis of the trends of the individual components of ΔE_{int} is given in the Supporting Information.

ΔE(SIBFA) reproduces ΔE(RVS) with relative errors in the 2−3.5% range. The numerical values of ΔE(RVS) obtained with the CEP 4-31G(2d) basis set are very close to those of ΔE(HF) obtained with the 6-311G** basis set. (In this comparison, however, the BSSE correction of ∼4 kcal/mol was subtracted automatically by the RVS procedure.) Such close numerical agreements were similarly noted in several studies of polycoordinated Zn complexes.[26b,30] The LACVP** basis set gives values that are uniformly 5% larger in absolute value than those obtained with the 6-311G** basis set, but the trends are identical. After addition of the contribution of E_{disp}/E_{corr}, ΔE_{int}(SIBFA) is seen to reproduce ΔE(MP2) with a relative error of 2−4%. The values of ΔE(DFT) obtained with the 6-311G** basis set are close to those of ΔE(MP2), which used the CEP 4-31G(2d) basis set, being numerically smaller by 6−11.2 kcal/mol out of 500, i.e., 2%. The LACVP** basis set gives values that are correspondingly larger by 5%. ΔE_{int}(SIBFA) is intermediate between the two DFT computations, except for complex (b), for which, due to the relative overestimation of E_{disp}, ΔE_{int}(SIBFA) has a slightly (2.3 kcal/mol) larger value than ΔE(DFT) obtained with the LACVP** set.

Similar close agreements between DFT and MP2 methods were also obtained for the complexes of $[Zn(H_2O)_5]^{2+}$ with guanine and adenine.[30] This should justify our use of DFT to study the larger 5′GMP$^-$ complexes, which are intractable by MP2. In general, DFT provides very good results for H-bonding and ionic complexes, comparable to MP2 data with medium basis sets of atomic orbitals and clearly superior to HF predictions. We have recently carried out reference RI-MP2/TZVPP calculations (equivalent to the MP2/cc-pVTZ level) for hydrated Mg^{2+} interacting with guanine and phosphate and concluded that the DFT method is in excellent agreement with the RI-MP2/TZVPP calculations.[56] Note, nevertheless, that DFT would not be suitable for van der Waals and stacking complexes.[57]

2. $[Zn(H_2O)_5]^{2+}$−5′GMP$^-$ Complexes. SIBFA Energy-Minimized Structures. Let us now introduce the calculations on the nucleotide complexes. The ribose sugar was held in either the C2′ or the C3′ endo conformation. For both conformers, arrangements **A**−**C**, defined above, were first energy-minimized using the SIBFA procedure, followed by single-point HF and DFT computations with both 6-311G** and LACVP** basis sets to ensure consistency of the results. The results are reported in Tables 2 and 3 for the C2′ and C3′ endo conformers, respectively. These tables report the values of ΔE_{int}(SIBFA) and its components, along with those of ΔE(HF) and ΔE(DFT) interaction energies. For the purpose of comparison with Mg(II) binding, we also report the ΔE_{int}(SIBFA) values after subtraction of the first-shell hydration energy of Zn(II), computed as the total interaction energy in the energy-minimized hexahydrate, $Zn^{2+}(H_2O)_6$, which amounts to −347.7 kcal/mol.[26] The corresponding interaction energies are denoted by ΔE_{int}*. The tables further show the values of the continuum solvation energies, ΔG_{solv}, as computed using the Langlet−Claverie method[33] within the SIBFA procedure and the Poisson−Boltzmann equation implemented in the Jaguar code in the framework of DFT.[35] The tables further give the conformational (intramolecular) energy differences, δE_{conf}, for the 5′GMP$^-$ monomer with respect to its most stable conformation, taken as energy zero. The latter was obtained by energy minimization

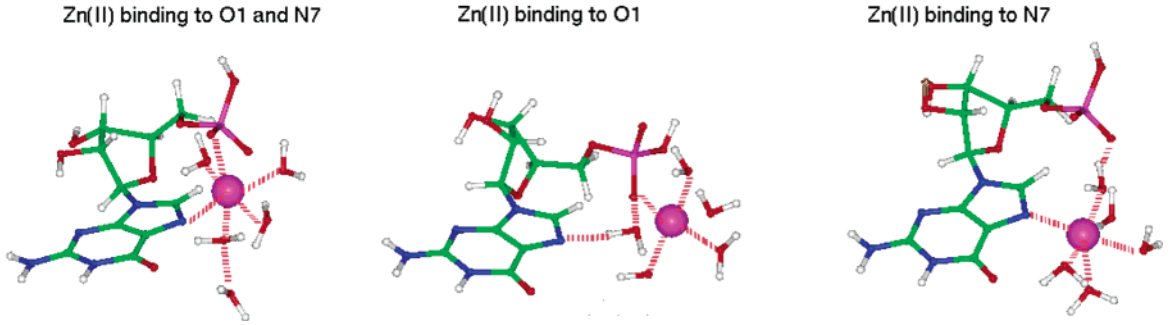

Figure 2. (a)−(c) Representation of the complexes of $[Zn(H_2O)_5]^{2+}$ with 5′GMP$^-$. Ribose in the C2′ endo conformation. SIBFA energy-minimized structures. (a) Simultaneous Zn(II) binding to O1 and N7. (b) Direct Zn(II) binding to O1. (c) Direct Zn(II) binding to N7.

TABLE 2: Complexes of 5′GMP$^-$ with $[Zn(H_2O)_5]^{2+}$ — HF, DFT, and SIBFA Computations Performed on the SIBFA Energy-Minimized Geometries (5′GMP$^-$ Ribose in the C2′ Endo Conformation)

	A	**B**	**C**
(a) Intermolecular Interaction Energies	N7 and O1	O1	N7
E_1	−418.6	−410.6	−386.1
E_{pol}	−83.3	−72.1	−106.9
E_{ct}	−27.0	−30.3	−30.9
E_2	−110.3	−102.3	−137.9
$\Delta E = E_1 + E_2$	**−528.9**	**−512.9**	**−524.0**
ΔE(HF) (i)[a]	**−536.1**	**−520.9**	**−527.3**
ΔE(HF) (ii)[b]	**−564.2**	**−550.1**	**−554.8**
E_{disp}	−58.2	−52.3	−59.4
ΔE_{int}(SIBFA)	**−587.1**	**−565.3**	**−583.3**
ΔE_{int}*(SIBFA)[c]	−239.4	−217.4	−235.6
ΔE(DFT) (i)	**−568.9**	**−554.3**	**−562.6**
ΔE(DFT) (ii)	**−602.3**	**−589.6**	**−594.5**
(b) Solvation Energies			
ΔG_{solv}(SIBFA)	−85.8	−94.1	−100.6
ΔG_{solv}(PB/DFT) (ii)	−84.6	−91.8	−93.9
(c) Isolated 5′GMP$^-$			
δE_{conf}(SIBFA)	13.5	12.3	15.6
δE_{conf}(DFT)[d] (i)	12.4	10.2	14.0
δE_{conf}(DFT) (ii)	12.0	10.6	14.8
ΔG_{solv}(SIBFA)	−106.7	−102.7	−104.7
ΔG_{solv}(PCM/DFT) (i)	−97.0	−101.0	−102.3
ΔG_{solv}(PB/DFT) (ii)	−114.8	−115.6	−117.5
(d) Relative Energies (Inter- Plus Conformational) of the Unsolvated Complexes			
δ(SIBFA)	0.0	20.6	5.9
δ(DFT) (i)	0.0	12.4	7.9
δ(DFT) (ii)	0.0	11.4	10.6

[a] (i), 6-311G** basis set. [b] (ii), LACVP** basis set. [c] After subtraction of the first-shell hydration energy of Zn^{2+}. [d] δE_{conf}(DFT) is computed with respect to the conformational energy of isolated 5′GMP$^-$ in its SIBFA-minimized conformation.

of isolated 5′GMP$^-$. Single-point HF and DFT computations were done on it in order to have the corresponding reference energy from the Q-C approaches.

The values of ΔG_{solv} of isolated 5′GMP$^-$ are similar to those of complexed 5′GMP$^-$. Partial energy balances, including the sum of ΔE_{int} and δE_{conf}, are also compared. ΔG_{solv} was not included in these balances, since the present energy minimizations were not done in the presence of solvation effects.

For C2′ endo sugar pucker (Table 2 and Figure 2), ΔE_{int}(SIBFA) ranks the complexes in the following order of stability: **A** > **C** > **B**. The same order is found by both DFT calculations. The numerical values of ΔE_{int}(SIBFA) are intermediate between the 6-311G** and the LACVP** DFT ones. The relative errors with respect to the Q-C interaction energies are 3.5%. It is very instructive to observe that the stabilization of complex **C**, in which Zn(II) binds directly to N7 and through-water to phosphate, is principally due to the polarization energy term, while E_1 has its least favorable values for this complex. ΔG_{solv}, obtained using the Langlet−Claverie approach, is seen to reproduce well ΔG_{solv} from the DFT computations using the Poisson−Boltzmann equation and its trends **C** > **B** > **A**. The lowest ΔG_{solv} values, found for **C**, reflect smaller mutual shielding of both the phosphate anionic charge and the Zn(II) cationic charge in **C** compared to **A** and **B**.

For uncomplexed 5′GMP$^-$, δE_{conf}(SIBFA) reproduces correctly δE_{conf} from the quantum-chemical computations, both at correlated and (not shown) uncorrelated levels. The SIBFA calculation of ΔG_{solv} underestimates ΔG_{solv}(DFT/PB) by ca. 10%, being closer to ΔG_{solv}(DFT/PCM). Further, it slightly favors complex **A**, contrary to both ΔG_{solv}(DFT) values.

The present shortcomings in SIBFA ΔG_{solv} computations could be a consequence of the present calibration of ΔG_{solv}. Refinements of the approach are underway which introduce an iterative coupling between the solvent reaction field and the solute-induced dipoles. It is to be noted, however, that the continuum model calculations of hydration energies are, in general, very sensitive to the parametrization, especially for non-neutral systems.

Finally, the partial energy balances, δ(SIBFA), in the absence of solvation give the same ordering of relative stabilities as the DFT computations, namely **A** > **C** > **B**, but δ(SIBFA) for complex **B** is larger than from DFT. This reflects the larger ΔE_{int}(SIBFA) energy difference between **B** and **A** (21.8 kcal/mol) compared with the DFT computations (15.6 and 13.7 kcal/mol with the two considered basis sets).

For C3′ endo complexes (Table 3 and Figure 3), ΔE_{int}(SIBFA) ranks the complexes again as **A** > **C** > **B**. ΔE_{int}(SIBFA) has values intermediate between the ΔE(DFT) ones obtained using the 6-311G** and LACVP** basis sets. The relative errors with respect to these two basis sets are 4.5 and 3%, respectively. ΔE_{int}(SIBFA) differs by similar amounts as ΔE(DFT) in the three complexes.

The conformational energies of isolated 5′GMP$^-$, δE_{conf}(SIBFA), are also in good agreement with the corresponding δE_{conf}(DFT) ones. The partial energy balances, δ(SIBFA), in the absence of solvation give again the same ordering, **A** > **C** > **B**, as from the DFT, and the magnitudes of δ(SIBFA) are now close to the corresponding δ(DFT) ones.

Similar observations can be made regarding the ΔG_{solv} values for both complexed and uncomplexed 5′GMP$^-$. Thus, for complexed 5′GMP$^-$, ΔG_{solv}(SIBFA) reproduces well ΔG_{solv}(DFT/PB) and its trends, while for uncomplexed 5′GMP$^-$ it has values intermediate between those from the two DFT approaches.

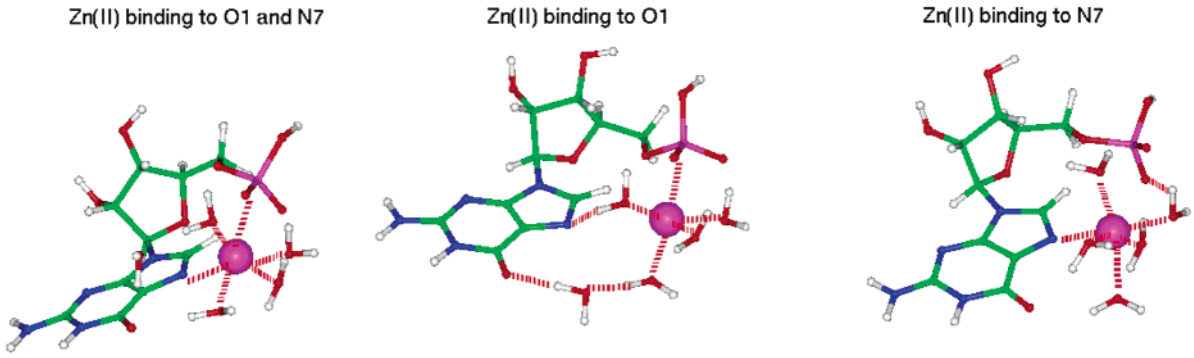

Figure 3. (a)−(c) Representation of the complexes of $[Zn(H_2O)_5]^{2+}$ with 5′GMP$^-$. Ribose in the C3′ endo conformation. SIBFA energy-minimized structures. (a) Simultaneous Zn(II) binding to O1 and N7. (b) Direct Zn(II) binding to O1. (c) Direct Zn(II) binding to N7.

3. $[Zn(H_2O)_5]^{2+}$−5′GMP^{-1} Complexes. Quantum-Chemical Energy-Minimized Structures. Next, the SIBFA energy-minimized structures of the six $Zn(H_2O)_5]^{2+}$−5′GMP$^-$ complexes presented above were used as starting points for HF gradient energy minimizations (see methods). To verify convergence of the investigations, the Q-C-optimized structures for complexes **A**−**C** were used as additional starting points for SIBFA reoptimization. Therefore, to ensure the stability of the SIBFA minima, and their actual closeness to the quantum-chemical ones, we have evaluated the mutual overlaps between three minima: the previous SIBFA optimizations marked as (p) structures, quantum-chemical (Q-C) geometries, and SIBFA geometries from the present restarts, (r). From the structural aspect, it was found that only limited variations of the ribose valence angles (<2°) occurred in the Q-C structures with respect to the standard unrelaxed values used in the SIBFA computations. The values of the ribose valence angles in the Q-C energy-minimized complexes **A**−**C** are reported in Table S2 (Supporting Information), along with the standard values used in the SIBFA computations. The sugar rings were found to have a close overlap with their starting structures, with rms deviations of 0.11 and 0.05 Å for C2′ endo and C3′ endo, respectively. The values of the backbone and glycosidic torsion angles of 5′GMP$^-$ that result from Q-C and SIBFA energy minimizations are reported in Tables S3 and S4 (Supporting Information). These tables concern 5′GMP$^-$ in isolation and in its most stable complex **A**, respectively.

Table S3 shows that, for the C2′ endo conformer, the SIBFA energy-minimized torsion angles can differ from the Q-C ones by up to 100° in the case of the C4′−C5′ torsion angle, and that the glycosidic angle is close to 0° in SIBFA, as compared to 55° from Q-C. A SIBFA energy minimization using the Q-C torsion angles as a starting point resulted into torsion angles much closer to the Q-C ones (except for the glysosidic angle) and a 3.1 kcal/mol higher than the δE_{conf} value. The energy-minimized Q-C and SIBFA torsional angles are much closer in the case of the C3′ endo sugar. Table S4 shows very similar torsional angle values from both Q-C and SIBFA approaches in the **A** complexes. Notably, the glycosidic angles always have very small amplitudes (<15°). With the C2′ endo sugar, the main changes undergone by 5′GMP$^-$ upon binding to the pentahydrate are related to the central P−O5′ and O5′−C4′ torsion angles. With both C2′ and C3′ endo sugars, these pass from 240−290° and 260° to 80° (g+) and 150° (t), respectively.

The energy results are reported in Table 4 for the C2′ endo complexes. For the SIBFA results, the values of ΔE_{int} in the previous minima (p) are reported along with the novel ones (r). The lowest ΔE_{int} value is underlined.

The three Q-C-relaxed C2′ endo complexes are represented in Figure 4, along with the corresponding SIBFA-restarted complexes. For all three complexes **A**−**C**, the restarted SIBFA minima structures give very close overlaps to the Q-C ones, with all heavy-atom rmsd's <0.6 Å. This implies that there are no major differences between these structures. For complexes **A** and **C**, the previous SIBFA complexes (p) are seen to overlap well with the Q-C ones (rmsd < 0.8 Å). On the other hand, for complex **B**, structure (p) has a significantly smaller overlap with the Q-C one (rmsd 1.5 Å), while the newly relaxed complex (r) overlaps much better (rmsd 0.6 Å). (r) also has an improved value of ΔE_{int}(SIBFA) relative to (p) (−578.5 versus −565.3 kcal/mol), while for complexes **A** and **C**, ΔE_{int} had more favorable values in the previous (p) structures.

The 6-311G** DFT interaction energies rank the three C2′ endo complexes along the sequence **A** > **B** > **C**. The differences

TABLE 3: Complexes of 5′GMP$^-$ with $[Zn(H_2O)_5]^{2+}$ − HF, DFT, and SIBFA Computations Performed on the SIBFA Energy-Minimized Geometries (5′GMP$^-$ Ribose in the C3′ Endo Conformation)

	A	**B**	**C**
(a) Intermolecular Interaction Energies	N7 and O1	O1	N7
E_1	−425.1	−390.1	−382.1
E_{pol}	−85.0	−91.8	−108.2
E_{ct}	−26.4	−33.8	−31.9
E_2	−111.5	−125.7	−140.1
$\Delta E = E_1 + E_2$	**−536.6**	**−515.8**	**−522.2**
ΔE(HF) (i)[a]	**−540.2**	**−511.6**	**−521.2**
ΔE(HF) (ii)[b]	**−568.7**	**−542.2**	**−551.4**
E_{disp}	−57.3	−58.7	−60.7
ΔE_{int}(SIBFA)	**−593.9**	**−574.5**	**−582.9**
ΔE_{int}*(SIBFA)[c]	−246.2	−226.8	−235.2
ΔE(DFT) (i)	**−572.5**	**−549.0**	**−558.0**
ΔE(DFT) (ii)	**−606.3**	**−584.8**	**−594.0**
(b) Solvation Energies			
ΔG_{solv}(SIBFA)	−83.4	−86.6	−96.5
ΔG_{solv}(PB/DFT) (ii)	−82.9	−84.7	−88.9
(c) Isolated 5′GMP$^-$			
δE_{conf}(SIBFA)	18.5	23.4	17.9
δE_{conf}(DFT)[d] (i)	22.2	20.3	18.4
δE_{conf}(DFT) (ii)	18.9	17.7	17.3
ΔG_{solv}(SIBFA)	−106.6	−103.1	−104.3
ΔG_{solv}(PCM/DFT) (i)	−96.8	−92.9	−99.0
ΔG_{solv}(PB/DFT) (ii)	−116.1	−113.7	−115.1
(d) Relative Energies (Inter- Plus Conformational) of the Unsolvated Complexes			
δ(SIBFA)	0.0	24.4	10.4
δ(DFT) (i)	0.0	21.7	10.9
δ(DFT) (ii)	0.0	20.3	10.7

[a] (i), 6-311G** basis set. [b] (ii), LACVP** basis set. [c] After subtraction of the first-shell hydration energy of Zn^{2+}. [d] δE_{conf}(DFT) is computed with respect to the conformational energy of isolated 5′GMP$^-$ in its SIBFA-minimized conformation.

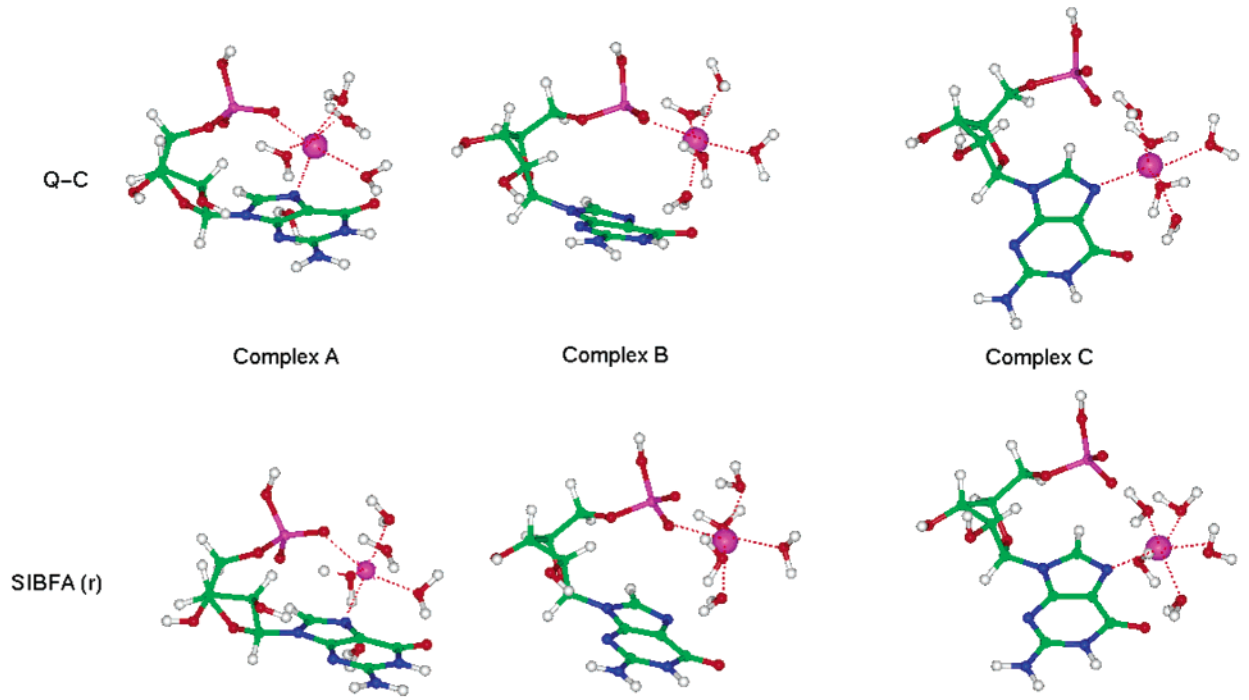

Figure 4. (a)−(c) Representation of the complexes of $[Zn(H_2O)_5]^{2+}$ with 5′GMP$^-$. Ribose in the C2′ endo conformation. Q-C energy-minimized structures. The conformations resulting from SIBFA restarts using these structures as starting points are also displayed. (a) Simultaneous Zn(II) binding to O1 and N7. (b) Direct Zn(II) binding to O1. (c) Direct Zn(II) binding to N7.

TABLE 4: Complexes of 5′GMP$^-$ (C2′ Endo Ribose) with $[Zn(H_2O)_5]^{2+}$ — HF, DFT, and SIBFA Computations[a]

	A	**B**	**C**
	Intermolecular Interaction Energies		
	N7 and O1	O1	N7
Δ*E*(DFT) (i)[b]	**−580.6**	**−576.7**	**−573.5**
Δ*E*(DFT) (ii)[c]	**−611.7**	**−612.8**	**−605.7**
SIBFA			
ΔE_{int} (r)[d]	**−584.3**	**−578.5**	**−574.2**
ΔE_{int} (p)[e]	**−587.0**	**−565.3**	**−583.3**
	Differences in Relative Total Energies (Including 5′GMP$^-$ Conformational Energy) with Respect to Complex **A**, Taken as Energy Zero		
DFT(i)	0.0	2.1	0.1
SIBFA			
(r)	0.4	4.9	15.4
(p)	0.0	20.9	6.9

rms Deviations (Å) on Heavy Atoms

	complex **A**			complex **B**			complex **C**		
	Q-C	(r)	(p)	Q-C	(r)	(p)	Q-C	(r)	(p)
Q-C	0.0	0.42	0.43	0.0	0.57	1.50	0.0	0.54	0.61
(r)	0.42	0.0	0.24	0.57	0.0	1.15	0.54	0.0	0.78
(p)	0.43	0.24	0.0	1.50	1.15	0.0	0.61	0.78	0.0

[a] The quantum-chemical computations are on the HF-gradient energy-minimized structures. The SIBFA computations (r) were resumed starting from the quantum-chemical computations. Also listed as (p) are the values from the independent SIBFA runs from Table 2. The rms deviations for the overlaps between the Q-C, r, and p minima are also listed. [b] (i), 6-311G** basis set. [c] (ii), LACVP** basis set.[d] (r), energy-minimized, restarted from quantum-chemical structure. [e] (p), previous SIBFA energy-minimized structure.

are small, however, less than 4 kcal/mol out of 580. The values of ΔE_{int}(SIBFA) retain the same ordering as in Table 2, namely **A** > **C** > **B**. The inversion in relative magnitudes of **B** and **C** takes place although the relative error of ΔE_{int}(SIBFA) with respect to ΔE_{int}(DFT) obtained with this basis set has decreased to 2%.

Upon including the intramolecular energy of 5′GMP$^-$, the 6-311G** calculations indicate the three complexes to differ by less than 2 kcal/mol in relative in vacuo stabilities. These energy differences are amplified in the SIBFA computations, the least stable complex, **C**, being 6.9 kcal/mol less stable than **A**. It is noted that the Q-C energy minimizations relax the valence angles and bond lengths of 5′GMP$^-$, in addition to its torsional angles, while the SIBFA energy minimizations relax only its torsional angles. Allowing for relaxation of the sugar puckering, and of some valence angles of 5′GMP$^-$, is envisaged as a forthcoming step in the SIBFA treatment of oligonucleotides. It will be interesting to see if additional flexibility with this treatment would reduce the differences in relative energies of these complexes.

The C3′ endo conformation calculations are shown in Table 5, and the complexes are represented in Figure 5. Upon resorting to the Q-C structures as new starting points for energy minimization, all three SIBFA minima (r) gave only slightly more favorable ΔE_{int} values than the initial ones. The overlaps with the corresponding Q-C structures are uniformly better than was the case with the C2′ endo conformers. The highest rmsd's occur for complex **B**, regarding mutually all three minima (p), Q-C, and (r). Rmsd's are nevertheless small (0.8 Å).

Δ*E*(DFT) obtained with the 6-311G** basis set ranks the complexes as **A** > **B** ≥ **C**. Single-point Δ*E*(DFT) obtained with the LACVP** basis set gives the ordering **A** > **C** ≥ **B**. As with the C2′ endo complexes, ΔE_{int}(SIBFA) is lower in complex **C** than in complex **B**, an inversion that takes place despite the reduction of relative error (2%) with respect to the Δ*E*(DFT) values obtained with the 6-311G** basis set. The DFT trends in total energies, including the intramolecular energy of 5′GMP$^-$, **A** > **C** > **B**, are correctly accounted for by SIBFA, but the energy differences are amplified. This may again reflect the need to introduce additional relaxation in the SIBFA calculations, in terms of sugar pucker and/or valence angle relaxation.

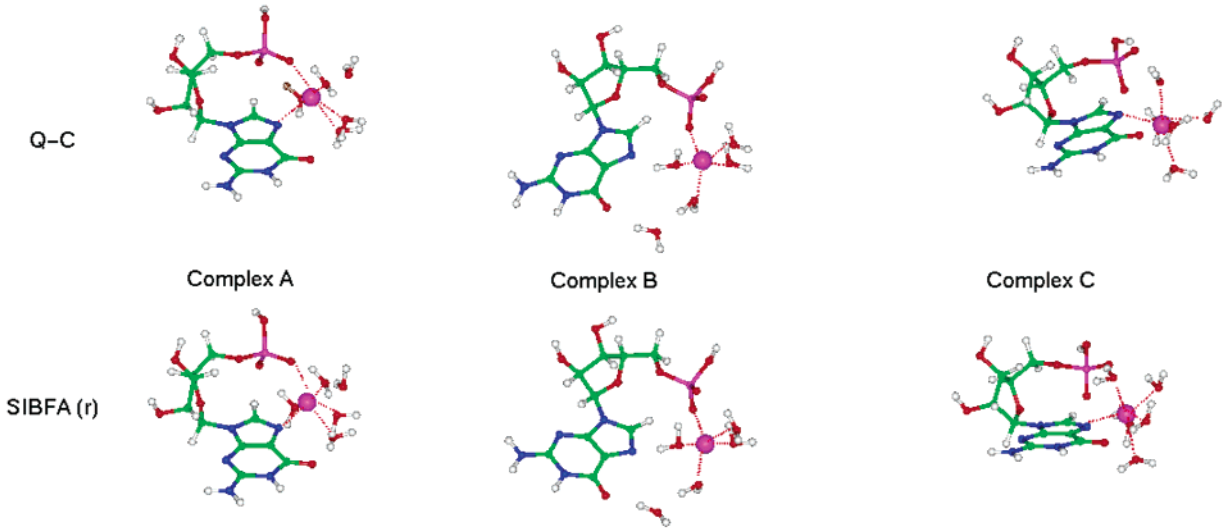

Figure 5. (a)−(c) Representation of the complexes of $[Zn(H_2O)_5]^{2+}$ with 5′GMP⁻. Ribose in the C3′ endo conformation. Q-C energy-minimized structures. The conformations resulting from SIBFA restarts using these structures as starting points are also displayed. (a) Simultaneous Zn(II) binding to O1 and N7. (b) Direct Zn(II) binding to O1. (c) Direct Zn(II) binding to N7.

TABLE 5: Complexes of 5′GMP⁻ (C3′ Endo Ribose) with $[Zn(H_2O)_5]^{2+}$ — HF, DFT, and SIBFA Computations[a]

	A	**B**	**C**
	Intermolecular Interaction Energies		
	N7 and O1	O1	N7
ΔE(DFT) (i)[b]	**−590.5**	**−578.9**	**−576.7**
ΔE(DFT) (ii)[c]	**−622.2**	**−607.3**	**−609.3**
SIBFA			
ΔE_{int} (r)[d]	**−595.8**	**−576.8**	**−584.4**
ΔE_{int} (p)[e]	**−593.8**	**−574.5**	**−583.1**
	Differences in Relative Total Energies (Including 5′GMP⁻ Conformational Energy) with Respect to Complex **A**, Taken as Energy Zero		
DFT (i)	0.0	8.2	5.8
SIBFA			
(r)	0.0	14.8	11.7
(p)	3.4	27.7	14.6

rms Deviations (Å) on Heavy Atoms

	complex **A**			complex **B**			complex **C**		
	Q−C	(r)	(p)	Q−C	(r)	(p)	Q−C	(r)	(p)
Q−C	0.0	0.25	0.42	0.0	0.47	0.82	0.0	0.53	0.75
(r)	0.25	0.0	0.27	0.47	0.0	0.78	0.53	0.0	0.66
(p)	0.42	0.27	0.0	0.82	0.78	0.0	0.75	0.66	0.0

[a] The quantum-chemical computations are on the HF-gradient energy-minimized structures. The SIBFA computations (r) were resumed starting from the quantum-chemical computations. Also listed as (p) are the values from the independent SIBFA runs from Table 2. The rms deviations for the overlaps between the Q-C, r, and p minima are also listed. [b] (i), 6-311G** basis set. [c] (ii), LACVP** basis set.[d] (r), energy-minimized, restarted from quantum-chemical structure. [e] (p), previous SIBFA energy-minimized structure.

Q-C and SIBFA computations consistently show that the C3′ endo sugar gives rise to more favorable ΔE_{int} values than the C2′ endo sugar for the best bound complexes **A**, when Zn(II) bridges both O1 and N7. With C3′ endo sugar, there is also a more accented preference favoring **A** complexes over **B** and **C** ones.

4. Mg(II) Binding. To obtain additional insights into metal−nucleotide interactions, we have carried out studies including Mg(II). For both C2′ and C3′ endo sugar puckers, SIBFA energy minimization was resumed starting from the best corresponding Zn complexes, which were regrouped in Table 5 above. Energy minimization was found to produce only minor rearrangements with respect to the corresponding Zn complexes. Single-point HF and DFT computations were then done at the minimized positions using both LAVCP** and 6-311G** basis sets. The results are reported in Table 6.

TABLE 6: Intermolecular Interaction Energies in the Complexes of 5′GMP⁻ with $[Mg(H_2O)_5]^{2+}$ — HF, DFT, and SIBFA Computations Performed on the SIBFA Energy-Minimized Geometries

	A	**B**	**C**
	5′GMP⁻ Ribose in the C2′ Endo Conformation		
	N7 and O1	O1	N7
E_1	−430.4	−433.0	−406.3
E_{pol}	−77.2	−69.0	−89.5
E_{ct}	−14.0	−18.8	−16.4
E_2	−91.2	−87.7	−105.9
$\Delta E = E_1 + E_2$	**−521.6**	**−520.7**	**−512.2**
ΔE(HF) (i)[a]	**−533.2**	**−529.5**	**−529.7**
ΔE(HF) (ii)[b]	**−561.9**	**−560.7**	**−558.2**
E_{disp}	−22.4	−22.6	−22.0
ΔE_{int}(SIBFA)	**−544.0**	**−543.3**	**−534.3**
ΔE_{int}*(SIBFA)[c]	−226.3	−225.6	−216.6
ΔE(DFT) (i)	**−537.1**	**−534.7**	**−535.5**
ΔE(DFT) (ii)	**−589.7**	**−590.5**	**−587.4**
	5′GMP⁻ Ribose in the C3′ Endo Conformation		
	O1 and N7	O1	N7
E_1	−440.4	−409.0	−397.4
E_{pol}	−78.6	−85.7	−100.7
E_{ct}	−13.5	−19.2	−19.2
E_2	−92.0	−104.8	−119.8
$\Delta E = E_1 + E_2$	**−532.4**	**−513.8**	**−517.2**
ΔE(HF) (i)	**−542.9**	**−512.3**	**−522.5**
ΔE(HF) (ii)	**−562.7**	**−542.9**	**−552.5**
E_{disp}	−22.0	−24.8	−26.0
ΔE_{int}(SIBFA)	**−554.3**	**−538.6**	**−543.2**
ΔE_{int}*(SIBFA)[c]	−236.6	−220.9	−225.5
ΔE(DFT) (i)	**−546.3**	**−519.8**	**−530.0**
ΔE(DFT) (ii)	**−598.1**	**−574.2**	**−584.1**

[a] (i), 6-311G** basis set. [b] (ii), LACVP** basis set. [c] After subtraction of the first-shell solvation energy of Mg^{2+}.

The Mg(II) complexes have ΔE_{int} values that are 38−44 kcal/mol smaller in absolute magnitudes than those in the corresponding Zn complexes. This difference stems from both E_2 and E_{disp} terms, while E_1 favors the Mg(II) complex. These trends are consistent with those previously observed upon comparing the binding energies of these two cations in model

hard and soft binding sites.[25d,26a,58] We note that, upon passing from the HF to the DFT level, the gain in ΔE_{int} is much smaller with the 6-311G** basis set (∼6 kcal/mol) than with the LACVP** basis set (∼30 kcal/mol). More significant energy gains, of ∼35 kcal/mol, were actually noted with both basis sets in the case of the corresponding Zn(II) complexes. The smaller stabilization gain due to correlation in the Mg complexes compared with the Zn ones is consistent with Mg(II) having a "hard" character, in contrast to the "soft" character of Zn(II).[59] However, we have no explanation for the larger reduction in the correlation energy gain that takes place with the 6-311G** basis set compared with the LACVP** one. At both uncorrelated and correlated levels, the SIBFA interaction energies are intermediate between the 6-311G** and LACVP** values, being much closer to the former, which they reproduce with relative errors <4%.

As pointed out by one reviewer, comparison of the binding affinities of Zn(II) and Mg(II) requires that we consider the differences between their ΔE_{int} values and their dehydration enthalpies. A meaningful estimate of the latter contribution can be provided by the corresponding differences of their first-shell hydration energies, namely the total interaction energies in the energy-minimized hexahydrates, $Zn^{2+}(H_2O)_6$ and $Mg^{2+}(H_2O)_6$. Such interaction energies, amounting to −347.7 and −317.7 kcal/mol, respectively,[26a] give a difference of 30 kcal/mol, which corresponds to the actual experimental difference of the enthalpies of hydration of these two cations.[60]

C2′ Endo Conformers. ΔE_{int}(SIBFA) and ΔE_{int}(DFT) obtained with both basis sets have closely similar values in complexes **A** and **B**. The situation with complex **C** is not very clear-cut; i.e., the structures are basically isoenergetic. Thus, **C** is disfavored with respect to **B** by both ΔE_{int}(SIBFA) and the LACVP** computations, but it is favored with respect to **B** by ΔE_{int}(DFT) obtained with the 6-311G** basis set.

The ΔE_{int}* values are obtained after the subtraction of the first-shell solvation energy of the divalent cation from ΔE_{int}. Comparing their values with the corresponding ones of Zn(II) in Table 2, we observe that ΔE_{int}* is invariably in favor of Zn(II) binding. The difference is the smallest (8.2 kcal/mol) in complex **B**, which is stabilized by direct cation binding to the phosphate O1 atom, and is the largest (19 kcal/mol) in complexes **C**, where the cations bind directly to the guanine N7 atom. It is intermediate (13 kcal/mol) in complex **A**, in which the cation binds simultaneously to O1 and N7. These trends appear consistent with the increased discrimination in favor of the "softer" Zn(II) cation over the "harder" Mg(II) due to the "softer" nitrogen ligand. They were previously discussed in related comparisons of the Zn(II) versus Mg(II) binding in metalloenzyme binding sites.[26a]

C3′ Endo Conformers. Consistent with the HF and DFT Q-C results, and now similar to the Zn(II) results, the SIBFA and both Q-C computations give the ordering of ΔE_{int} values: **A** > **C** > **B**. The values of ΔE_{int} in the best-bound complex **A** are also lower with a C3′ endo than with a C2′ endo sugar pucker. This implies the C3′ endo sugar pucker to be more prone to the bridging of O1 and N7 by a divalent cation than the C2′ endo pucker. Comparing the ΔE_{int}* values with the corresponding ones of Zn(II) in Table 3, we observe that, as was the case for the C2′ endo complexes, the difference favoring Zn(II) over Mg(II) is the smallest (5.9 kcal/mol) in complex **B**. This energy difference amounts to 9.6 kcal/mol for both **A** and **C** binding modes.

5. Comparison with Other Polarizable Molecular Mechanics Potentials. As pointed out by a reviewer, it is of interest to compare the present results with those from other polarizable molecular mechanics, notably AMBER 7.0.[61] In the absence of available AMBER 7.0 parameters for Zn(II), we have accordingly reinvestigated, for both C2′ and C3′ endo conformers, complexes **A**−**C** of 5′GMP$^-$ with the Mg(II) pentahydrate. For comparison purposes, the calculations were done with both the polarizable ff02 and the nonpolarizable ff99 force fields. The net charge on the Mg cation was 2+, as in the SIBFA computations. We have reported in Table S5 (Supporting Information) the ff99 and ff02 results, first at the SIBFA minima and then after a full relaxation. The ΔE_{int}(AMBER) values were, similar to the SIBFA and Q-C ones, computed as the difference between the total energy of the complex and the energies of the individual monomers at their geometries and conformations in the complex.

C2′ Endo Conformer. At the starting positions, the values of the AMBER ΔE_{int}(ff02) computed for complexes **A**−**C** are very close to the SIBFA ones, namely −545.3, −538.5, and −533.5 kcal/mol, respectively, as compared to −544.0, −543.3, and −534.3 kcal/mol in SIBFA. The numerical agreement is worse with the ff99 force field (−507.3, −500.6, and −489.6 kcal/mol in **A**−**C**). The values of E_{pol}(ff02) also have a good correspondence with those from SIBFA, namely, for **A**−**C**, respectively −71.8, −74.2, and −87.2 kcal/mol with AMBER and −77.2, −69.0, and −89.5 kcal/mol with SIBFA. Energy minimization, however, resulted in large increases of the ff02 interaction energies, which became −618.5, −625.4, and −644.5 kcal/mol in **A**−**C**, respectively. Thus, complex **C**, with Mg(II) bound through water to O1, is now the one endowed with the lowest ΔE_{int} value, due to its significantly lower E_{pol} component (−124.1 kcal/mol as compared to −79.8 and −86.5 kcal/mol in **A** and **B**). On the other hand, the ff99 force field gives, following energy minimization, complexes **A** and **B** as more stable than **C**, by a larger energy difference (18 kcal/mol) than SIBFA (9 kcal/mol). The fact that E_{pol} is lowest for **C** is fully consistent with our previous SIBFA and ab initio results that bore on the complexes of formate[54] and phosphate (see above) with the pentahydrates of the Zn(II) cation. These results had shown that complexes with indirect, water-mediated binding of the divalent cation to the anion (as is the case with complex **C**) were those with the lowest values of the polarization energy. With respect to direct binding modes, however, the amount of relative stabilization due to E_{pol} did not exceed 20 kcal/mol, that is, about twice as small as with the present ff02 results. Examination of the structure of complex **C** after ff02 energy minimization showed that the two water molecules mediating the O1−Mg(II) interaction had extremely short distances between one of their H atoms and O1, namely 1.13 and 1.21 Å. These distances are much shorter than the shortest corresponding H−O1 distances from the other procedures, which are 1.55 Å (Q-C), 1.69 Å (SIBFA), and 1.53 Å (ff99). They are probably indicative of overpolarization effects due to nonadditivity; that is, the shorter the H−O1 distances, the lower the value of E_{pol} in the ternary phosphate−water−Mg(II) complexes. The formulation and calibration of E_{pol}(SIBFA) were done by referring to energy decomposition results that bore on representative monoligated complexes of divalent cations.[25a] It was found that the shielding of the electrostatic field exerted by the cation with a distance-dependent function enabled us to reproduce the behavior of E_{pol}(RVS) on all investigated complexes. In light of the present findings, we would like to propose a similar shielding to be tested in AMBER for the modeling of the complexes of divalent cations.

Conclusions and Perspectives

We have carried out structural and energy calculations of key binding modes of hydrated Zn(II) and Mg(II) cations to 5′-guanosine monophosphate, the basic building block of nucleic acids. Our study includes bidentate binding of the dication to O1 and N7 (denoted as complex **A**) and monodentate binding to either O1 (denoted as complex **B**) or N7 (complex **C**), along with through-water binding to the other atom. Each of the two predominant sugar puckers occurring in DNA and RNA, C2′ endo and C3′ endo, was considered. The calculations were carried out by advanced polarizable molecular mechanics (PMM) approach SIBFA, computing the interaction energy as a sum of five separate components. The PMM SIBFA approach, in contrast to common molecular modeling force fields, properly includes all contributions to molecular interactions, such as polarization and charge transfer, and is uniquely designed to treat metal cation−biopolymer interactions. On the other side, it is much faster than quantum-chemical calculations and breaks the interactions into individual contributions, which is of primary importance to rationalize the diversity of metal cation binding to DNA and RNA. While permanent multipoles are used to compute the first-order electrostatic component, E_{MTP}, the inclusion into ΔE_{int} of explicit E_{pol} and E_{ct} components should enable us to address the multipole transferability issue that occurs upon building a large molecule from rigid fragments[62] and account for the effects of charge fluctuations that occur in DNA and RNA as functions of conformation and environment.[63] To account for the interplay of inter- and intramolecular polarization and charge-transfer effects that occur simultaneously in complexes involving flexible molecule such as 5′GMP$^-$ with the Zn and Mg pentahydrates, we resorted to a newly developed approach. All interfragment interactions are computed simultaneously, and the interaction energy, ΔE_{int}, and its components are derived after subtraction of the summed interfragment interactions occurring within uncomplexed 5′GMP$^-$ in the conformation it has in the complex. The separable nature of the SIBFA potential sheds light on those energy components of ΔE_{int} that preferentially stabilize binding of different cations to different binding sites. The SIBFA calculations are extensively compared with ab initio quantum-chemical data.

Assuming the C3′ endo conformation, ΔE_{int} (SIBFA) was found to favor complex **A** by much larger energy differences (>9 kcal/mol) than with the C2′ endo conformation. For C2′ endo, the interaction energy gap between complexes **A** and **B** is in the range of 2.5−4 kcal/mol out of 600. There was a full agreement between SIBFA and DFT computations in this respect. Complex **A**, with bidentate binding of the dication to 5′GMP$^-$, was found to give rise to more favorable ΔE_{int} values with the sugar in the C3′ endo conformation than in a C2′ endo conformation. For the Zn(II) pentahydrate, the values of ΔE_{int}-(SIBFA) remained consistently intermediate between those of ΔE(DFT) as computed with two basis sets, 6-311G** and LACVP**, which they reproduced with relative errors of 4%. For both C2′ endo and C3′ endo conformers, complex **C**, with through-water Zn or Mg binding to phosphate, had much more favorable E_{pol} values than either complex **A** or **B**. This surprising result shows that the reduction of intermolecular polarization energy of the phosphate in the through-water mode is overcompensated for by its reduced screening due to the field exerted by the dication on N7 and by local cooperative effects in M(II)−water−phosphate arrangements.

On the basis of the above data, we can conclude that the accuracy of the SIBFA procedure for this kind of interactions is within the error margins of medium-level DFT ab initio calculations. Further, SIBFA provides a correct balance of the individual interaction components and allows reliable decomposition of the interactions over a wide range of binding motifs and for different metal cations.

We have further carried out gradient HF energy minimizations with the 6-31G* basis set using the SIBFA energy-minimized structures as starting points. For full consistency, the HF minima in turn served as a starting point for a second SIBFA energy minimization, to ensure that relevant minima had not been missed. There was a close overlap between the best minima from SIBFA and ab initio minima, with an rmsd on heavy atoms <1 Å.

Upon computing the conformational (intramolecular) energies of isolated 5′GMP$^-$, δE_{conf}, we found it necessary to resort to the multipoles of the elementary fragments of methyl phosphate taken in isolation rather than to the multipoles of the integral anion, because this would otherwise lead to severe imbalances of δE_{conf} for some conformations. This was due to the corresponding imbalance of the fragment−fragment interactions taking place within this anion. We have interpreted this finding by the fact that the multipoles in integral methyl phosphate embody the effects of electronic redistribution due to the mutual interactions between its fragments which took place during the SCF process. Computing the interfragment interactions with these multipoles leads to double-counting. On the other hand, constructing methyl phosphate with mutually interacting, elementary constitutive fragments, and accounting for the energetical effects of electronic redistribution by the E_{pol} and E_{ct} terms, is in line with the conclusions of our previous studies, which addressed the issue of conformation dependence of the interaction energies.[28b,39,41a,b] Such a construction was found to allow for a good reproduction of the corresponding δE_{conf} values from Q-C calculations. The issue of multipole transferability was raised for the first time for oligopeptides.[62] In light of the present findings, it could be important to resort to comparisons with Q-C results to evaluate how a related issue regarding the phosphodiester group can be handled in the context of other PMM procedures. From a recent review paper,[64] it appears that, while ab initio conformational analysis of nucleosides has now been thoroughly investigated, extensions to actual nucleotides, such as 5′GMP$^-$, are presently limited.

The present calculations, besides proving the ability of SIBFA PMM to deal with the metal−DNA interactions, also give several interesting insights into the metal−nucleotide interactions. Partial energy balances, which took into account the differences in dehydration energies of Zn(II) and Mg(II), indicated more favorable interaction energies for $[Zn(H_2O)_5]^{2+}$ than $[Mg(H_2O)_5]^{2+}$. The preferences were the largest in complexes **C** and the smallest in complexes **A**. They stemmed from the E_2 and E_{disp} components, while E_1 favored Mg(II), consistent with the "softer" character of Zn(II) compared to Mg(II). This would imply that 5′GMP$^-$ would bind Zn(II) more favorably than Mg(II), particularly when N7 is involved, and this appears to be in agreement with available experimental data.[11c] It should be noted, however, that a complete analysis of the cation binding preferences would require analysis of larger systems and consideration of the solvation effects. The balance of different terms is the source of different properties of these two cations, despite their equal charge and almost equal radii. The present results are in line with analyses in model binding sites in proteins[26a] and rationalize preceding ab initio studies of metal binding to N7 of guanine.[22c] SIBFA clearly shows that the stabilization of complex **C**, in which Zn(II) or Mg(II) binds

directly to N7 and through-water to phosphate, is principally due to the polarization energy term.

In the case of the Mg(II) complexes, we have also done computations using the polarizable ff02 force field in AMBER 7.0.[61] The ΔE_{int} values had good agreement with the corresponding DFT and SIBFA ones in single-point computations at the SIBFA energy-minimized structures. However, energy minimization with ff02 resulted into too large a stabilization of complex **C** over complexes **A** and **B**, contrary to the DFT and SIBFA results. This was due to the polarization contribution. In the energy-minimized complex **C**, there was an exaggerated shortening of the hydrogen bonds between the anionic phosphate oxygen O1 and the two water molecules interposed between O1 and Mg(II), the H−O1 distances being 1.13 and 1.21 Å. This translated local overpolarization in the ternary Mg(II)−water−phosphate complexes. This could possibly be remedied by screening the polarizing field in the ff02 force field with the help of an exponential or a Gaussian function.

We have also reported comparisons between the solvation free energies, ΔG_{solv}, computed with the Langlet et al. continuum reaction field and ΔG_{solv} data from Poisson−Boltzmann and polarizable charge model computations within the DFT framework. We have thus compared ΔG_{solv} for uncomplexed, monoanionic 5′GMP$^-$ (with its geometry frozen as in the six complexes with hydrated zinc) with those for the six monocationic complete complexes. While for the monocationic complexes ΔG_{solv} reproduced ΔG_{solv}(PB) with a relative error of 5%, the difference increased to 12% in the case of uncomplexed 5′GMP$^-$. On the other hand, the absolute values of ΔG_{solv}(SIBFA) were consistently intermediate between the PB and those from PCM calculations. There are no precedents to our knowledge for comparisons between ΔG_{solv} from polarizable molecular mechanics and ΔG_{solv} from DFT computations bearing on nucleotides, whether in isolation or complexed. Along with results recently obtained for models for Zn-finger binding sites,[29] the present data stimulate refinements to ΔG_{solv}, which are presently underway. These include an iterative coupling between the solvent reaction field and the solute-induced dipoles and will be reported elsewhere.

Acknowledgment. The quantum-chemical computations reported by N.G. were done on the computers of the Institut du Développement en Ressources Informatiques (IDRIS), 91405 Orsay, and the Centre de Ressources Informatiques de Haute-Normandie (CRIHAN), 76800 St. Etienne-du-Rouvray. Additional calculations were carried out at the Mississippi Center for Supercomputer Research. This work was supported by grants LN00A016, MSMT CR (J.S., J.E.S., N.S.), NSF grant CREST 9805465 (J.E.S., J.S., J.L.), NIH grant RCMI G1 2RR13459-21 (J.L.), and a Wellcome Trust Senior Research Fellowship for Biomedical Research in Central Europe GR067507 (J.S., N.S.).

Supporting Information Available: Analysis of the trends of individual interaction energy components in complexes (a)−(d); tables listing valence bond angles, torsion angles, and total ineraction energies and their components for complexes **A**−**C**. This material is available free of charge via the Internet at http://pubs.acs.org.

References and Notes

(1) Holbrook, S. R.; Sussman, J. L.; Warrant, R. W.; Church, G. M.; Kim, S. H. *Nucleic Acids Res.* **1977**, *4*, 2811.

(2) (a) Scott, W. G.; Murray, J. B.; Arnold, J. R. P.; Stoddard, B. L.; Klug, A. *Science* **1996**, *274*, 2065. (b) Pley, H. W.; Flaherty, K. M.; McKay, D. B. *Nature* **1994**, *372*, 68.

(3) Cate, J. H.; Hanna, R. L.: Doudna, J. A. *Nature Struct. Biol*. **1997**, *4*, 553.

(4) Wedekind, J. E.; McKay, D. B. *Nature Struct. Biol***. 1999**, *6*, 261.

(5) (a) Valadkhan, S.; Manley, J. L. *Nature Struct. Biol*. **2002**, *9*, 498. (b) Huppler, A.; Niskstad, L. J.; Allman, A. M.; Brow, D. A.; Butcher, S. E. *Nature Struct. Biol*. **2002**, *9*, 431.

(6) Egli, M.; Minasov, G.; Su, L.; Rich, A. *Proc. Natl. Acad. Sci. U.S.A.* **2002**, *99*, 4302.

(7) (a) Correll, C. C.; Freeborn, B.; Moore, P. B.; Steitz, T. A. *Cell* **1997**, *91*, 705. (b) Lu, M.; Steitz, T. A. *Proc. Natl. Acad. Sci. U.S.A.* **2000**, *97*, 2023.

(8) (a) Nixon, P. L.; Giedroc, D. P. *Biochemistry* **1998**, *327*, 16116. (b) Gonzalez, R. L.; Tinoco, I. *J. Mol. Biol*. **1999**, *289*, 1267.

(9) (a) Breaker, R. R.; Joyce, G. F. *Chem. Biol*. **1994**, *1*, 223. (b) Lu, Y. *Chem. Eur. J*. **2002**, *8*, 4589.

(10) Lipscomb, W. N.; Strater, N. *Chem. Rev.* **1996**, *96*, 2375. (b) Wilcox, E. A. *Chem. Rev.* **1996**, *96*, 2435.

(11) (a) Bernues, J.; Beltran, R.; Casasnovas, J. M.; Azorin, F. *EMBO J*. **1989**, *8*, 2087. (b) Cherny, D. I.; Malkov, V. A.; Volodin, A. A.; Frank-Kamenetskii, M. D. *J. Mol. Biol.* **1993**, *230*, 379. (c) Potaman, V. N.; Soyfer, V. N. *J. Biomol. Struct. Dyn*. **1994**, *11*, 1035.

(12) Khomyakova, E. B.; Gousset, H.; Liquier, J.; Huynh-Dinh, T.; Gouyette, C.; Takahashi, M.; Florentiev, V. L.; Taillandier, E. *Nucleic Acids Res*. **2000**, *18*, 3511.

(13) Bernues, J.; Beltran, R.; Casasnovas; J. M.; Azorin, F. *Nucleic Acids Res*. **1991**, *19*, 1633.

(14) McFail-Isom, L.; Shui, X. Q.; Williams, L. D. *Biochemistry* **1998**, *37*, 17105.

(15) (a) Sponer, J.; Sponer, J. E.; Leszczynski, J. *J. Biomol. Struct. Dyn.* **2000**, *17*, 108. (b) Petrov, A. S.; Lamm, G.; Pack, G. R. *J. Phys. Chem. B* **2002,** *106*, 3294.

(16) Cheatham, T. E. I.; Young, M. A. *Biopolymers* **2000,** *56*, 23.

(17) McConnell, K. J.; Beveridge, D. L. *J. Mol. Biol.* **2000**, *304*, 80.

(18) (a) Csaszar, K.; Spacková, N.; Stefl, R.; Sponer, J.; Leontis, N. B. *J. Mol. Biol.* **2001**, *313*, 1073. (b) Reblova, K.; Spackova, N.; Stefl, R.; Csaszar, K.; Koca, J.; Leontis, N. B.; Sponer, J. *Biophys. J.* **2003**, *84*, in press.

(19) (a) Spackova, N.; Berger, I.; Sponer, J. *J. Am. Chem. Soc.* **1999**, *121*, 5519. (b) Spackova, N.; Berger, I.; Sponer, J. *J. Am. Chem. Soc.* **2001**, *123*, 3295. (c) Chowdhury, S.; Bansal, M. *J. Phys. Chem. B* **2001**, *105*, 7572.

(20) Hermann, T.; Auffinger, P.; Scott, W. G.; Westhof, E. *Nucleic Acids Res.* **1997**, *25*, 3421.

(21) Elizondo-Riojas, M. A.; Kozelka, J. *J. Mol. Biol***. 2001,** *314*, 1227.

(22) (a) Ross, W. S.; Hardin, C. C. *J. Am. Chem. Soc.* **1994**, *116*, 6070. (b) Sponer, J.; Leszczynski; J.; Hobza, P. *Biopolymers* **2002**, *61*, 3. (c) Sponer, J.; Burda, J. V.; Sabat, M.; Leszczynski, J.; Hobza, P. *J. Phys. Chem. A* **1998**, *102*, 5951.

(23) Haider, S.; Parkinson, G. N.; Neidle, S. *J. Mol. Biol***. 2002,** *320*, 189.

(24) Halgren, T. A.; Damm, W. *Curr. Opin. Struct. Biol*. **2001**, *11*, 236.

(25) (a) Gresh, N.; Claverie, P.; Pullman, A. *Theor. Chim. Acta* **1984**, 66. (b) Gresh, N.; Claverie, P.; Pullman, A. *Int. J. Quantum Chem*. **1986**, *29*, 101. (c) Gresh, N. *J. Comput. Chem.* **1995**, *16*, 856. (d) Gresh, N.; Garmer, G. *J. Comput. Chem*. **1996**, *17*, 1481.

(26) (a) Garmer, D.; Gresh, N.; Roques, B. P. *Proteins* **1998**, *31*, 42. (b) Tiraboschi, G.; Gresh, N.; Giessner-Prettre, C.; Pedersen, L. G.; Deerfield, D. W. *J. Comput. Chem*. **2000**, *21*, 1011.

(27) (a) Gresh, N. *J. Phys. Chem. A* **1997**, *101*, 8680. (b) Masella, M.; Gresh, N.; Flament, J. P. *J. Chem. Soc., Faraday Trans*. **1998**, *94*, 2745. (c) Guo, H.; Gresh, N.; Roques, B. P.; Salahub, D. R. *J. Phys. Chem. B* **2000**, *105*, 9746.

(28) (a) Gresh, N.; Roques, B. P. *Biopolymers* **1997**, *41*, 145. (b) Antony, J.; Gresh, N.; Olsen, L.; Hemmingsen, L.; Schofield, C.; Bauer, R. *J. Comput. Chem*. **2002**, *23*, 1281.

(29) Gresh, N.; Derreumaux, P. *J. Phys. Chem. B* **2003**, *108*, 4862.

(30) Gresh, N.; Sponer, J. *J. Phys. Chem. B* **1999**, *104*, 11415.

(31) Sponer, J.; Sabat, M.; Gorb, L.; Leszczynski, J.; Lippert, B.; Hobza, P. *J. Phys. Chem. B* **2000**, *104*, 7535.

(32) (a) Tsui, V.; Case, D. A. *J. Am. Chem. Soc*. **2000**, *122*, 2489. (b) Tsui, V.; Case, D. A. *J. Phys. Chem. B* **2001**, *105*, 11314.

(33) Langlet, J.; Claverie, P.; Caillet, J.; Pullman, A. *J. Phys. Chem*. **1988**, *92*, 1631.

(34) Langlet, J.; Gresh, N.; Giessner-Prettre, C. *Biopolymers* **1995**, *36*, 765.

(35) Tannor, D. J.; Marten, B.; Murphy, R.; Friesner, R. A.; Sitkoff, D.; Nicholls, A.; Ringnalda, M.; Goddard, W. A., III; Honig, B. *J. Am. Chem. Soc*. **1994**, *116*, 11875.

(36) Tomasi, J.; Persico, M. *Chem. Rev*. **1994**, *94*, 2027.

(37) Vigné-Maeder, F.; Claverie, P. *J. Chem. Phys.* **1988**, *88*, 4934.

(38) Garmer, D. R.; Stevens, W. J. *J. Phys. Chem*. **1989**, *93*, 8263.

(39) Gresh, N.; Shi, G. B. *J. Comput. Chem***. 2003**, *24*, 000.

(40) Stevens, W. J.; Basch, H.; Krauss, M. *J. Chem. Phys*. **1984**, *81*, 6026.

(41) (a) Rogalewicz, F.; Ohanessian, G.; Gresh, N. *J. Comput. Chem.* **2000**, *21*, 963. (b) Tiraboschi, G.; Fournié-Zaluski, M. C.; Roques, B. P.; Gresh, N. *J. Comput. Chem.* **2001**, *22*, 1038. (c) Ren, P.; Ponder, J. W. *J. Comput. Chem*. **2002**, *23*, 1497.

(42) Evangelakis, G. A.; Rizos, J. P.; Lagaris, I. E.; Demetropoulos, I. N. *Comput. Phys. Commun.* **1987**, *46*, 401.

(43) Stevens, W. J.; Fink, W. *Chem. Phys. Lett.* **1987**, *39*, 15.

(44) Cammi, R.; Hofmann, H.-F.; Tomasi, J. *Theor. Chim. Acta* **1989**, *76*, 297.

(45) Pople, J. A.; Binkley, J. S.; Seeger, R. *Int. J. Quantum Chem. Symp.* **1976**, *10*, 1.

(46) Schmidt, M. W.; Baldridge, K. K.; Boatz, J. A.; Elbert, S. T.; Gordon, M. S.; Jensen, J. H.; Koseki, S.; Matsunaga, N.; Nguyen, K. A.; Su, S.; Windus, T. L.; Dupuis, M.; Montgomery, J. A., Jr. *J. Comput. Chem.* **1993**, *14*, 1347.

(47) (a) Lee, C.; Yang, W.; Parr, R. G. *Phys. Rev.* **1988**, *B37*, 785. (b) Becke, A. D. *J. Chem. Phys.* **1993**, *98*, 5648.

(48) Hay, P. J.; Wadt, W. R. *J. Chem. Phys.* **1985**, *82*, 299.

(49) Frisch, M. J.; Trucks, G. W.; Schlegel, H. B.; Scuseria, G. E.; Robb, M. A.; Cheeseman, J. R.; Zakrzewski, V. G.; Montgomery, J. A., Jr.; Stratmann, R. E.; Burant, J. C.; Dapprich, S.; Millam, J. M.; Daniels, A. D.; Kudin, K. N.; Strain, M. C.; Farkas, O.; Tomasi, J.; Barone, V.; Cossi, M.; Cammi, R.; Mennucci, B.; Pomelli, C.; Adamo, C.; Clifford, S.; Ochterski, J.; Petersson, G. A.; Ayala, P. Y.; Cui, Q.; Morokuma, K.; Malick, D. K.; Rabuck, A. D.; Raghavachari, K.; Foresman, J. B.; Cioslowski, J.; Ortiz, J. V.; Stefanov, B. B.; Liu, G.; Liashenko, A.; Piskorz, P.; Komaromi, I.; Gomperts, R.; Martin, R. L.; Fox, D. J.; Keith, T.; Al-Laham, M. A.; Peng, C. Y.; Nanayakkara, A.; Gonzalez, C.; Challacombe, M.; Gill, P. M. W.; Johnson, B.; Chen, W.; Wong, M. W.; Andres, J. L.; Gonzalez, C.; Head-Gordon, M.; Replogle, E. S.; Pople, J. A. *Gaussian 98*, Revision A.6; Gaussian, Inc.: Pittsburgh, PA, 1998.

(50) Jaguar 4.1, Schrodinger Inc., Portland, OR, 2000.

(51) Hurley, M. M.; Pacios, L. F.; Christiansen, P. A.; Roos, R. B.; Ermler, W. C. *J. Chem. Phys.* **1986**, *84*, 6840.

(52) Since for such comparisons we did not compute the intramolecular interactions between the methyl phosphate fragments, we used here the multipolar expansion of the whole molecule rather than those of its isolated fragments.

(53) Pullman, B.; Pullman, A.; Berthod, H. *Int. J. Quantum Chem. Symp.* **1978**, *5*, 79.

(54) Tiraboschi, G.; Roques, B. P.; Gresh, N. *J. Comput. Chem*. **1999**, *20*, 1379.

(55) Dubois, C.; Archirel, P.; Boutin, A. *J. Phys. Chem. B* **2001**, *105*, 9363.

(56) Rulisek. L.; Sponer, J. *J. Phys. Chem. B* **2003**, *107*, 1913.

(57) (a) Kristyan, S.; Pulay, P. *Chem. Phys. Lett.* **1994**, *229*, 175. (b) Hobza, P.; Sponer, J.; Reschel, T. *J. Comput. Chem*. **1995**, *16*, 1315. (c) Perez-Jorda, J. M.; san-Fabian, E.; Perez-Jimenez, A. J. *J. Chem. Phys*. **1999**, *110*, 1916. (d) Wesolowski, T. A.; Parisel, O.; Ellinger, Y.; Weber, J. *J. Phys. Chem. A* **1997**, *101*, 7818.

(58) Garmer, D. R.; Gresh, N. *J. Am. Chem. Soc*. **1994**, *116*, 3556.

(59) (a) Parr, R. G.; Pearson, R. G. *J. Am. Chem.* **1983**, *105*, 7512. (b) Pearson, R. G. *J. Am. Chem. Soc*. **1988**, *110*, 7684.

(60) Halliwell, H. F.; Nyburg, S. C. *Trans. Faraday Soc.* **1963**, *59*, 1126.

(61) (a) Wang, J.; Cieplak, P.; Kollman, P. A. *J. Comput. Chem*. **2000**, *21*, 1049−1074. (b) Case, D. A.; Pearlman, D. A.; Caldwell, J. W.; Cheatham, T. E., III; Wang, J.; Ross, W. S.; Simmerling, C. L.; Darden, T. A.; Merz, K. M.; Stanton, R. V.; Cheng, A. L.; Vincent, J. J.; Crowley, M.; Tsui, V.; Gohlke, H.; Radmer, R. J.; Duan, Y.; Pitera, J.; Massova, I.; Seibel, G. L.; Singh, U. C.; Weiner, P. K.; Kollman, P. A. AMBER 7, University of California, San Francisco, 2002.

(62) Faerman, C. H.; Price, S. L. *J. Am. Chem. Soc*. **1990**, *112*, 4915.

(63) Khandogin, J.; York, D. M. *J. Phys. Chem. B* **2002,** *106*, 7693.

(64) Foloppe, N.; Nilsson, L.; MacKerell, A. D., Jr. *Biopolymers* **2002**, *61*, 61.